

Simulation of Ultra-High Energy Photon Propagation with PRESHOWER 2.0

P. Homola^{a,*}, R. Engel^b, A. Pysz^a, H. Wilczyński^a

^a*H. Niewodniczański Institute of Nuclear Physics, Polish Academy of Sciences,
ul. Radzikowskiego 152, 31-342 Kraków, Poland*

^b*Karlsruhe Institute of Technology, 76021 Karlsruhe, Germany*

Abstract

In this paper we describe a new release of the PRESHOWER program, a tool for Monte Carlo simulation of propagation of ultra-high energy photons in the magnetic field of the Earth. The PRESHOWER program is designed to calculate magnetic pair production and bremsstrahlung and should be used together with other programs to simulate extensive air showers induced by photons. The main new features of the PRESHOWER code include a much faster algorithm applied in the procedures of simulating the processes of gamma conversion and bremsstrahlung, update of the geomagnetic field model, and a minor correction. The new simulation procedure increases the flexibility of the code so that it can also be applied to other magnetic field configurations such as, for example, encountered in the vicinity of the sun or neutron stars.

Keywords:

ultra-high energy cosmic rays, extensive air showers, geomagnetic cascading, gamma conversion, PRESHOWER

*Corresponding author: Tel.: +48 12 6628348; fax: +48 12 6628012.
Email address: Piotr.Homola@ifj.edu.pl (P. Homola)

1. Program Summary

Program title:	PRESHOWER 2.0
Catalog identifier:	ADWG_v2_0
Program summary URL:	http://cpc.cs.qub.ac.uk/summaries/ADWG_v2_0.html
Program obtainable from:	CPC Program Library, Queen's University, Belfast, N. Ireland
Licensing provisions:	Standard CPC licence, http://cpc.cs.qub.ac.uk/licence/licence.html
Programming language:	C, FORTRAN 77
Computer(s) for which the program has been designed:	Intel-Pentium based PC
Operating system(s) for which the program has been designed:	Linux or Unix
RAM required to execute with typical data:	< 100 kB
CPC Library Classification:	1.1.
External routines/libraries used:	IGRF [1, 2], DBSKA [3], ran2 [4]
Catalog identifier of previous version:	ADWG_v1_0
Journal Reference of previous version:	Computer Physics Communications 173 (2005) 71-90
Does the new version supercede the previous version?:	yes
Nature of problem:	Simulation of a cascade of particles initiated by UHE photon in magnetic field.
Solution method:	The primary photon is tracked until its conversion into an e^+e^- pair. If conversion occurs each individual particle in the resultant preshower is checked for either bremsstrahlung radiation (electrons) or secondary gamma conversion (photons).
Reasons for the new version:	1) Slow and outdated algorithm in the old version (a significant speed up is possible); 2) Extension of the program to allow simulations also for extraterrestrial magnetic field configurations (e.g. neutron stars) and very long path lengths.

Summary of revisions:

A veto algorithm was introduced in the gamma conversion and bremsstrahlung tracking procedures. The length of the tracking step is now variable along the track and depends on the probability of the process expected to occur. The new algorithm reduces significantly the number of tracking steps and speeds up the execution of the program. The geomagnetic field model has been updated to IGRF-11, allowing for interpolations up to the year 2015. Numerical Recipes procedures to calculate modified Bessel functions have been replaced with an open source CERN routine DB-SKA. One minor bug has been fixed.

Restrictions:

Gamma conversion into particles other than an electron pair is not considered. Spatial structure of the cascade is neglected.

Running time:

100 preshower events with primary energy 10^{20} eV require a 2.66 GHz CPU time of about 200 sec.; at the energy of 10^{21} eV, 600 sec.

2. Introduction

Identifying and understanding the sources of cosmic rays with energies up to 10^{20} eV is one of the most important questions in astroparticle physics (see, for example, [5, 6, 7]). Knowing the fraction of photons in the flux of ultra-high energy cosmic rays is of particular importance as photons are unique messengers of particular source processes (acceleration vs. decay of super-heavy particles or other objects). They are also produced in interactions of charged cosmic ray nuclei of the highest energies with cosmic microwave background radiation, known as the Greisen-Zatsepin-Kuzmin (GZK) effect. If the energy of the cosmic ray particles exceeds the GZK energy threshold at the source, ultra-high energy photons are produced due to well-understood hadronic interactions with microwave photons and can be detected at Earth as a unique propagation signature. So far only upper limits to the photon flux at ultra-high energy exist, which have led to severe constraints on models for UHECR sources. However, depending on the primary cosmic ray composition, the sensitivity of the latest generation of cosmic ray detectors, i.e. the Pierre Auger Observatory [8] and the Telescope Array [9], should allow detection of GZK photons for the first time.

The simulation of the propagation of photons before they reach the Earth's atmosphere is important because of the preshower effect [10] that may occur when a photon traverses a region where the geomagnetic field component transverse to the photon trajectory is particularly strong. As described e.g. in Refs. [11, 12], high energy photons in the presence of a magnetic field may convert into e^+e^- pairs and the newly created leptons emit bremsstrahlung photons, which again may convert into e^+e^- if their energies are high enough. As a result of these interactions, instead of a single high energy photon, a shower of particles of lower energies, the so-called preshower, reaches the atmosphere. The occurrence of the preshower effect has a large impact on the subsequent extensive air shower development and changes the predicted shower observables.

In 2005 the program PRESHOWER [11] for simulating the showering of photons in the Earth's magnetic field was released. It was shown that this initial version of the Monte Carlo code is in good general agreement with previous studies [10, 13, 14, 15, 16, 17, 18]. In this paper we describe the changes of the PRESHOWER code relative to the initial version 1.0 [11]. The main feature of the new release is a much faster algorithm for calculating the distance at which a preshower interaction (gamma conversion or

bremsstrahlung) occurs. In version 1.0, the calculations were done in constant steps along the particle trajectory and the step size was optimized for all possible trajectories. The constant step practically disabled studying the preshower effect along paths longer than several tens of thousands kilometers. Now, in version 2.0, the distance to the next interaction point is computed with an efficient veto algorithm, decreasing significantly the number of computing steps. The new method, being independent of the trajectory length, allows computations for arbitrarily long photon paths, e.g. simulations of preshower creation in the vicinity of a neutron star or active galactic nucleus. The new algorithm is described in detail in Section 3 of this article. Other important changes, i.e. the update of the geomagnetic field model and a code correction in version 1.0 are discussed in Section 4. The results of testing PRESHOWER 2.0 are presented in Section 5 and conclusions are given in Section 6.

Following Ref. [11], all the results presented in the following are obtained for the magnetic conditions of the Pierre Auger Observatory in Malargüe, Argentina (35.2°S, 69.2°W). The shower trajectories are given in the local frame where the azimuth increases in the counter-clockwise direction and $\phi = 0^\circ$ refers to a shower coming from the geographical North.

3. The new sampling algorithm

In PRESHOWER 1.0 the effect of precascading is simulated following the particle trajectories with a fixed step size. In each step the probability of conversion into e^+e^- is calculated for photons and the probability of emitting a bremsstrahlung photon is computed for electrons. The step size has to be optimized for all possible trajectories and magnetic field configurations encountered along the particle trajectories. It has been found out that a step size of 10 km works well until the primary photon conversion and then the emission of bremsstrahlung photons as well as conversions of secondary photons are simulated in steps of 1 km. In this algorithm a typical simulation run consists of several thousands of steps.

The number of simulation steps and hence the computing time can be significantly reduced by using a veto algorithm. The algorithm used in the following is commonly applied in physical situations where a probability of occurring of a certain process varies within a given spatial or temporal interval (see, e.g. Ref. [19]). The location or time of the occurrence of a physical process studied is found in few approximating jumps. An example of a pro-

cess that can be treated with the algorithm is a radioactive decay considered in a certain interval of time. Photon conversion and bremsstrahlung probabilities to be found along spatial trajectories can also be computed with this veto algorithm.

3.1. General description

The theory behind the veto algorithm is based on a process of discrete events described by

$$\frac{dN}{dt} = -f(t) N(t). \quad (1)$$

Then the probability dP_A of occurrence of process A in the time window $t \dots t + dt$ is given by

$$dP_A = -\frac{1}{N(t)} \frac{dN}{dt} = f(t) dt. \quad (2)$$

Together with the probability of not having an occurrence of process A in the time from t_0 to t

$$P_{\text{no-}A} = \frac{N(t)}{N(t_0)} \quad (3)$$

one obtains for the probability dP for having an occurrence of A in the time window $t \dots t + dt$, provided that this process did not occur at an earlier time t' with $t_0 < t' < t$

$$dP = P_{\text{no-}A} dP_A = f(t) \frac{N(t)}{N(t_0)} dt = f(t) \exp \left\{ - \int_{t_0}^t f(t') dt' \right\} dt. \quad (4)$$

If an analytic solution can be found for the integral of $f(t)$

$$F(t) = \int_{t_0}^t f(t') dt' \quad (5)$$

one can sample the time t of the next occurrence of A after the previous occurrence at time t_0 using the inversion method

$$\int_{t_0}^t dP = \exp\{F(t)\} = \xi, \quad t = F^{-1}(\ln \xi), \quad (6)$$

with ξ being a random number uniformly distributed in $(0, 1]$.

If $F(t)$ cannot be found or the inverse of it computed sufficiently easily one can use a function $g(t)$ such that $\forall t \geq 0 : g(t) \geq f(t)$ and apply the following procedure

1. set the initial conditions: $i = 0, t_0 = 0$;
2. $i = i + 1$;
3. get a random number $\xi_i \in (0, 1)$;
4. compute $t_i = G^{-1}(G(t_{i-1}) - \ln \xi_i)$, $t_i > t_{i-1}$;
5. get another random number $\xi'_i \in (0, 1)$;
6. if $\xi'_i \leq f(t_i)/g(t_i)$ then t_i is the wanted result, i.e. the moment when process A occurred, otherwise one has to go back to step 2 or, if the end of the interval is reached, end the procedure without occurrence of process A .

The algorithm described above was mathematically proven to reproduce exactly the expected distributions [20].

3.2. Implementation in PRESHOWER 2.0

Following the general scheme described above, the application of the veto algorithm to simulations of the preshower effect is straightforward. Instead of the time variable t , the distance r along the preshower trajectory is used. We consider two processes in parallel over an interval starting at r_{start} and ending at r_{end} , namely gamma conversion and bremsstrahlung of electrons. Following the physics notation introduced in Ref. [11] (see also the Appendices A and B for all the required physics formulas and symbols) the probability functions are defined as

$$p_{conv}(r) \equiv \alpha(\chi(r)) \quad (7)$$

(see Eqs. A.1-A.5) for gamma conversion and

$$p_{brem}(r) \equiv \int_0^E I(B_{\perp}(r), E, h\nu) \frac{d(h\nu)}{h\nu} \quad (8)$$

(see Eqs. B.1-B.7) for magnetic bremsstrahlung. The function $f(t)$ is then replaced by $p_{conv}(r)$ or $p_{brem}(r)$, depending on the process to be simulated. Since finding the antiderivatives of $p_{conv}(r)$ or $p_{brem}(r)$ is not straightforward, simple functions limiting $p_{conv}(r)$ and $p_{brem}(r)$ are used. We define

$$\begin{aligned} g_{conv}(r) &\equiv p_{conv}^{max} = const, \quad \forall r \in (r_{start}, r_{end}) : p_{conv}^{max} \geq p_{conv}(r), \\ g_{brem}(r) &\equiv p_{brem}^{max} = const, \quad \forall r \in (r_{start}, r_{end}) : p_{brem}^{max} \geq p_{brem}(r), \end{aligned} \quad (9)$$

which replace $g(t)$ and for which the antiderivatives are

$$\begin{aligned} G_{conv}(r) &= p_{conv}^{max} \cdot r, \\ G_{brem}(r) &= p_{brem}^{max} \cdot r. \end{aligned} \quad (10)$$

With these substitutions the algorithm of Sec. 3.1 is applied in PRESHOWER 2.0 for the two interaction processes.

The determination of $p_{conv/brem}^{max}$ is crucial for computing time optimization. Too large $p_{conv/brem}^{max}$ increases the total number of steps to be executed in the procedure.

3.3. Determination of $p_{conv/brem}^{max}$

The functions $p_{conv/brem}(r)$ depend on $B_{\perp}(r)$, which is computed with a numerical model. Hence finding the absolute maxima p_{conv}^{max} and p_{brem}^{max} is done numerically. Moreover, through the dependence on $B_{\perp}(r)$, both $p_{conv}(r)$ and $p_{brem}(r)$ depend on the primary arrival direction and the geographical location of the observatory. As can be seen in Figs. 1 and 2, the values of p_{conv}^{max} and p_{brem}^{max} may be significantly different for various arrival directions.

This indicates that the computation of p_{conv}^{max} and p_{brem}^{max} should be performed for each trajectory separately, otherwise one would have to apply upper limits of these values which would be universal but excessively large for most directions. Accepting the excessive values of $p_{conv/brem}^{max}$ would increase enormously the number of steps in the veto algorithm and might result in an unacceptable increase of the computing time.

Typically, the functions $p_{conv}(r)$ and $p_{brem}(r)$ reach their global maximum at the top of the atmosphere, i.e. at the end of preshower simulations, assumed here to be at the altitude of 112 km. This is the point closest to the Earth's surface and $B_{\perp}(r)$ typically reaches the maximum value. However for certain classes of trajectories $B_{\perp}(r)$ might start to decrease with approaching the geomagnetic field source when the trajectory direction approaches a tangent to the local field lines. If this decrease happens to be close to the Earth surface, preshower particles are exposed to the maximum $B_{\perp}(r)$ somewhere before reaching the atmosphere. Examples of p_{conv}^{max} and p_{brem}^{max} with local extrema are plotted in Figs. 1 and 2. The positions of the minima of $p_{conv/brem}(r)$ are closely correlated with the minima of $B_{\perp}(r)$.

In case of $p_{conv}(r)$, it has been checked that its global maximum is well reproduced by computing the function value along the trajectory in a simple loop with steps of 1000 km. This procedure is performed for the primary photon energy and the trajectory of interest. It has been checked that $p_{conv}(r)$ decreases with energy, so p_{conv}^{max} found for the primary photon energy will work also for secondary photons of lower energies. In case of electrons, $p_{brem}(r)$ may increase with decreasing electron energy, so one has to compute p_{brem}^{max} for energies within the entire energy range of the simulated particles. Here p_{brem}^{max}

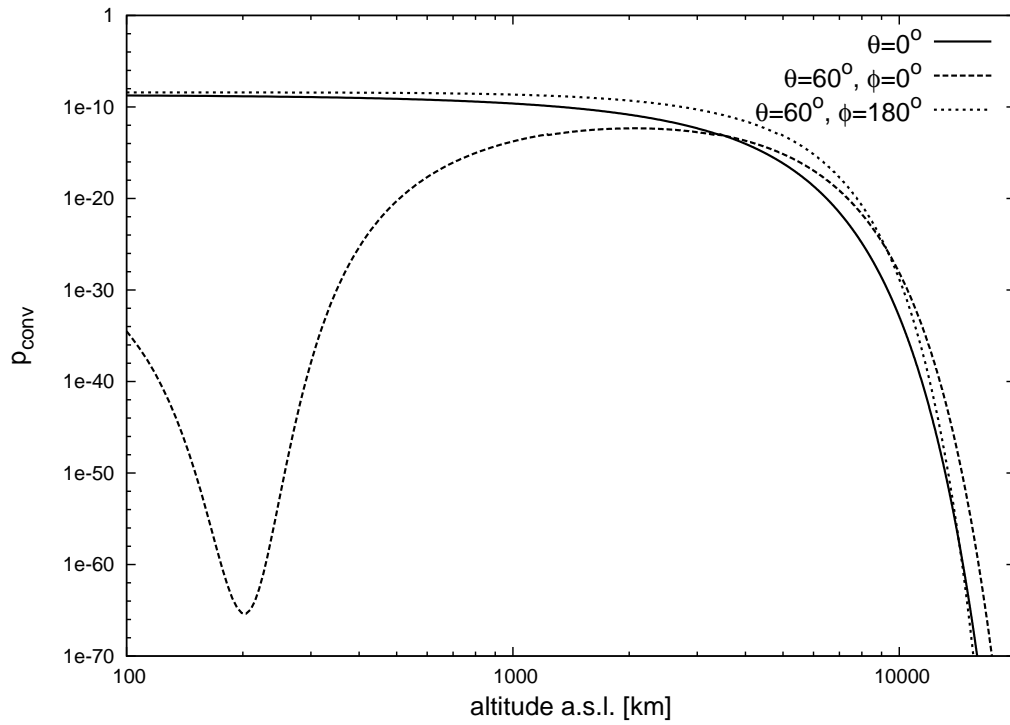


Figure 1: Examples of p_{conv} functions along different trajectories at the location of the Pierre Auger Observatory in Malargüe (Argentina). A minimum value for one of the curves is related to the small value of B_{\perp} for this specific arrival direction and altitude. See text for further details.

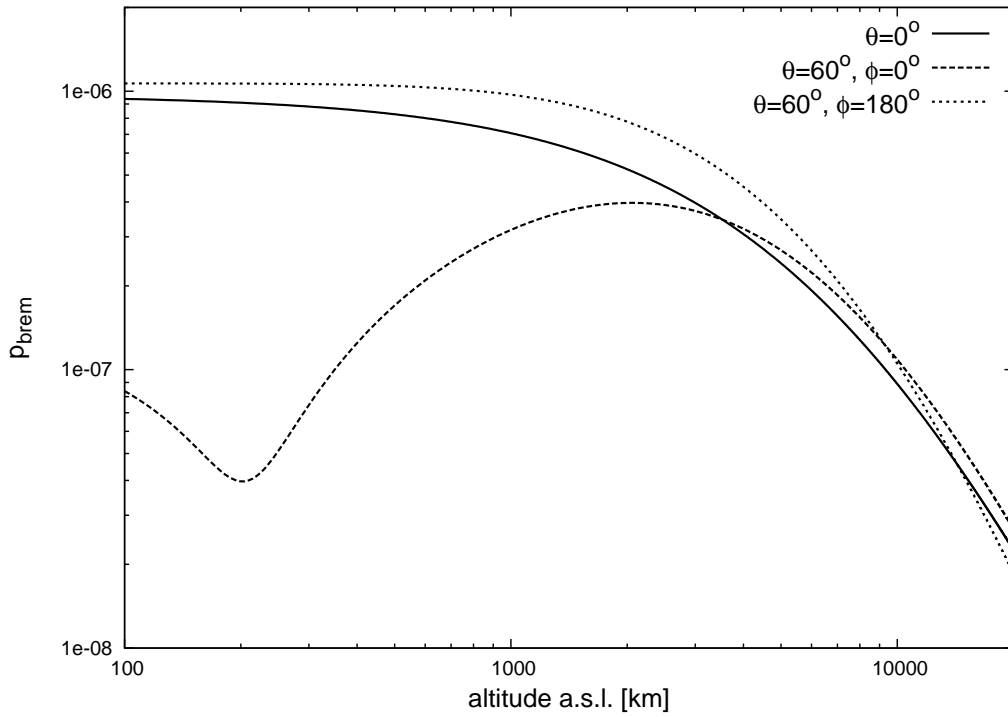


Figure 2: Examples of p_{brem} functions along different trajectories at the location of the Pierre Auger Observatory in Malargüe (Argentina). A minimum value for one of the curves is related to the small value of B_{\perp} for this specific arrival direction and altitude. See text for further details.

is computed in two loops. The external loop along the trajectory is done in steps of 1000 km and the internal loop over energies decreases the energy by one decade in each step. The steps in both procedures can be adjusted by the user if necessary. There is also an alert in the program that gets triggered when the actual values of $p_{conv/brem}(r)$ happen to exceed $p_{conv/brem}^{max}$.

The above method of finding the absolute maxima of $p_{conv/brem}(r)$ is fast and efficient. However, it is optimized only for specific simulation conditions: preshowering in the geomagnetic field. In other environments, involving more irregular shapes of $B(r)$, one has to reconsider the procedure of finding the absolute maxima of $p_{conv/brem}(r)$.

4. Other modifications and corrections

Other modifications and changes applied in the new release of the PRESHOWER program are briefly listed below.

1. The IGRF geomagnetic field model has been updated to the year 2010 and the most recent IGRF-11 coefficients have been applied (Ref. [21]). In the updated model, the highest order of spherical harmonics has been increased from 10 to 13. The geomagnetic field can be extrapolated up to the year 2015 with the new model. The differences between the field strength and direction in these two models are not larger than 0.001%.
2. Procedures to calculate modified Bessel functions have been replaced with an open source CERN routine DBSKA.
3. A minor problem has been found in the auxiliary function `kappa(x)` used for calculation of bremsstrahlung probability. The interpolation performed in this function failed for the rare case of $x = 10.0$. This happened because of a faulty definition of the last interval where the interpolation was done. As a result of this bug the input value $x = 10.0$ was excluded from the computations. This bug has been fixed in the new release of the program.
4. Since for some cases the number of preshower particles can be very large, the size of the array `part_out[50000][8]`, which stores the output particle data, has been increased from 50000 to 100000 entries.
5. The code of the program was reorganized and more clearly structured. The main change here was moving the auxiliary functions and routines to a separate file.

A list of the new and modified files with basic explanations can be found in the Appendix C.

5. Validation of the new version

The new release has been intensively tested. Below we show some examples to illustrate the performance.

In Fig. 3 a comparison of conversion probability obtained with PRESHOWER 1.0 and PRESHOWER 2.0 is presented for different arrival directions and primary energy of 7×10^{19} eV. The lines represent conversion probabilities obtained by numerical integrations of the expression (A.5) along trajectories and with steps as given in PRESHOWER 1.0. The points are plotted to show fractions of events with gamma conversion simulated by PRESHOWER 2.0. Each fraction was calculated after 10,000 simulation runs. Simulations of gamma conversion probabilities for other primary energies has also been checked and in all cases an excellent agreement between the results of the two PRESHOWER versions has been found.

A cross-check of the procedures responsible for simulation of bremsstrahlung is shown in Fig. 4, in which the energy distribution of secondary particles for a primary photon of 10^{20} eV and an arrival direction along which the transverse component of the geomagnetic field is particularly strong (“strong field direction”) are compared. Plotted are the summed distributions of energies of secondary photons and electrons together with the relevant histograms weighted by the energies. The summations are done for 500 simulation runs. The results obtained with the two program versions are in very good agreement.

Further tests for the same set of simulations are shown in Figs. 5 and 6. These are the number of preshower particles and the total energy carried by the preshower electrons. Both observables are calculated at the top of the atmosphere and both are plotted versus the altitude of primary photon conversion. In both figures a comparison is made between the results obtained with PRESHOWER 1.0 and PRESHOWER 2.0. Again, the agreement between the results of the two PRESHOWER versions is very good.

One of the main aims of the new release of PRESHOWER was to reduce the computing time. The results of the CPU time comparison are summarized in Table 1. The computing time is more than a factor 5 shorter in case of simulations with PRESHOWER 2.0 than in the case of PRESHOWER 1.0. This reduction is seen both in computation of gamma conversion (speed up by nearly factor 10) and in more time consuming bremsstrahlung routines.

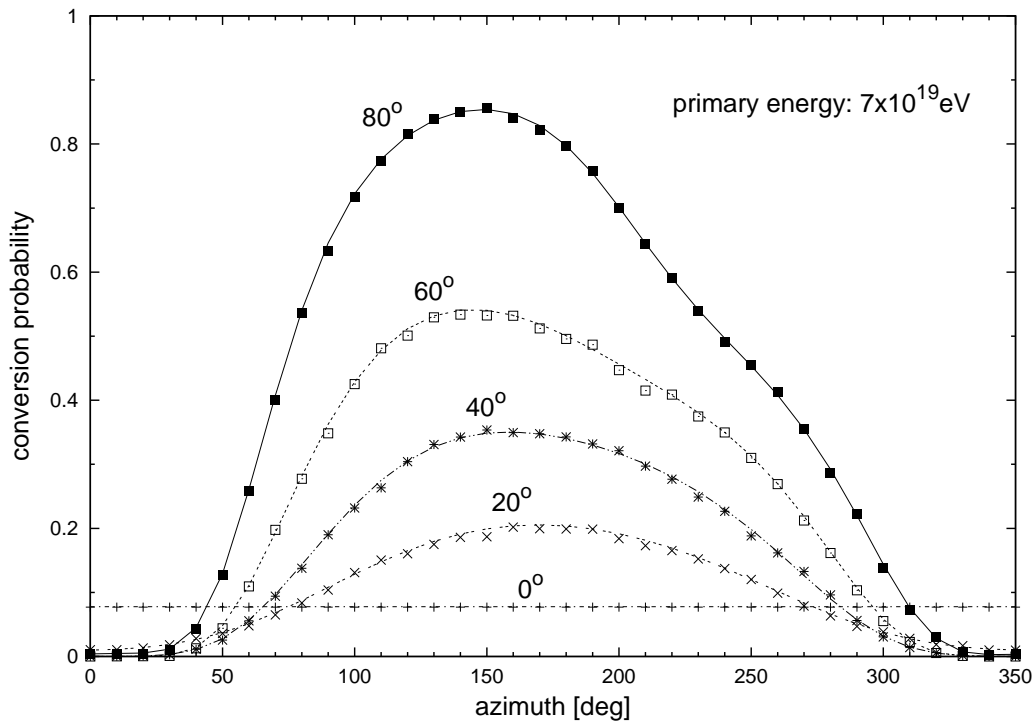


Figure 3: Total probability of γ conversion for the primary energy of 7×10^{19} eV for different arrival directions as computed by PRESHOWER 1.0 (lines) and PRESHOWER 2.0 (points). PRESHOWER 1.0 values were obtained by numerically integrating the conversion probability in the loop over trajectory. The points represent the fractions of events with gamma conversion simulated by PRESHOWER 2.0 with the new veto algorithm. Each fraction is the average for 10000 primary photons. Computations have been done for magnetic conditions at the Pierre Auger Observatory in Argentina. The azimuth 0° refers to showers arriving from the geographic North.

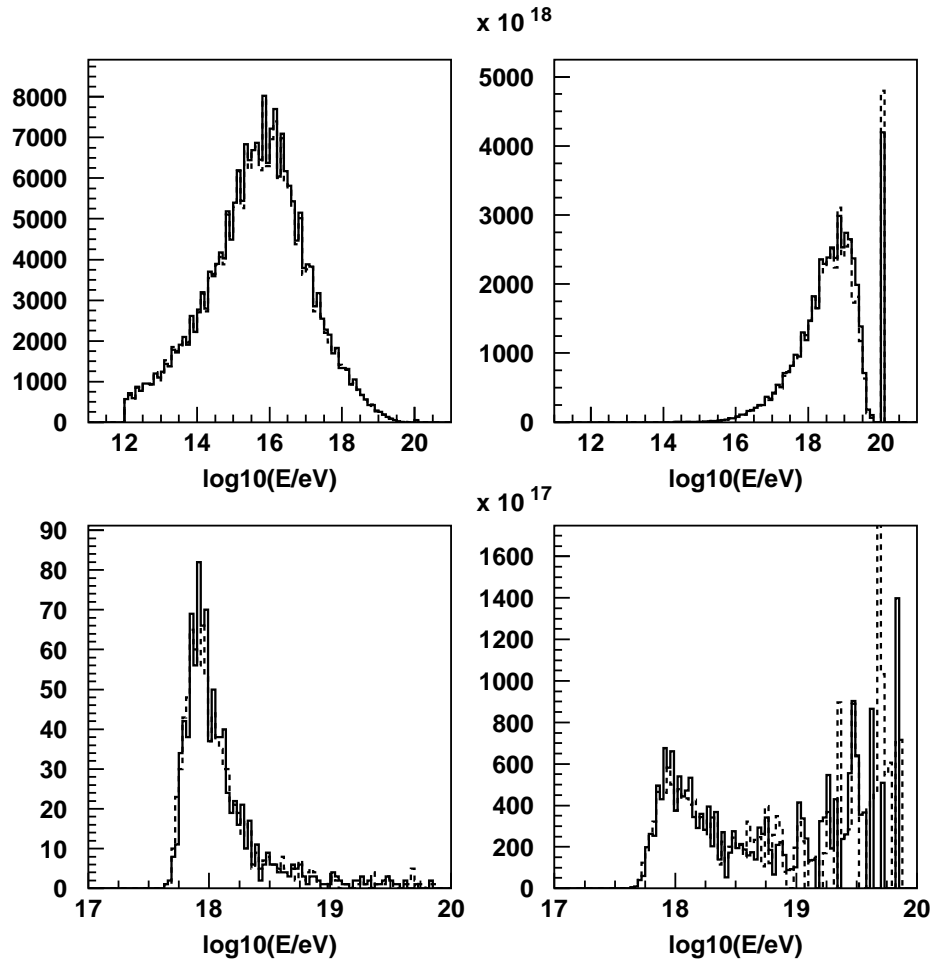


Figure 4: Energy distribution of photons (top left) and electrons (bottom left) in 500 preshowers initiated by 10^{20} eV photons arriving at the Pierre Auger Observatory in Argentina from the strong field direction. The spectra weighted by energy are plotted to the right. The dashed histograms were obtained with PRESHOWER 1.0 and the solid ones with PRESHOWER 2.0.

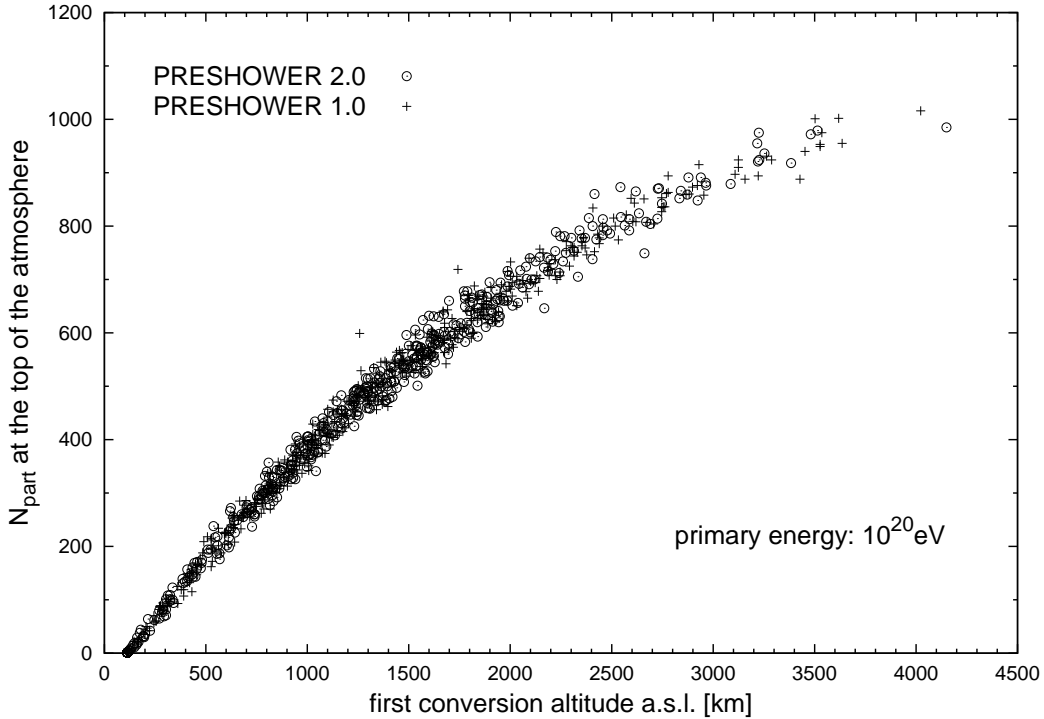


Figure 5: Number of particles in the preshower for different altitudes of the first γ conversion simulated with PRESHOWER 1.0 and PRESHOWER 2.0. Plotted are the preshowers initiated by 10^{20} eV photons arriving from the strong field direction. The two points somewhat higher than those of the general trend are cases where one of the bremsstrahlung photons again converted in the magnetic field to produce an electron-positron pair which emitted the additional photons. See also Fig. 6.

Table 1: The preshower simulation times in PRESHOWER 1.0 (old) and PRESHOWER 2.0 (new) for selected arrival directions and primary energies. The arrival directions are selected to represent a typical variation of B_{\perp} : $\theta = 70^{\circ}$ and $\phi = 0^{\circ}$ for a “weak” B_{\perp} , $\theta = 0^{\circ}$ for a “medium” B_{\perp} and $\theta = 60^{\circ}$ and $\phi = 177^{\circ}$ for a “strong” B_{\perp} .

E_0 [eV]	direction	fraction of converted	time [sec.]	old time [sec.]	new time [sec.]
7×10^{19}	$\theta = 0^{\circ}$	0/1000	79	7	
7×10^{19}	$\theta = 70^{\circ}, \phi = 0^{\circ}$	0/1000	76	8	
10^{20}	$\theta = 60^{\circ}, \phi = 177^{\circ}$	92/100	1195	209	

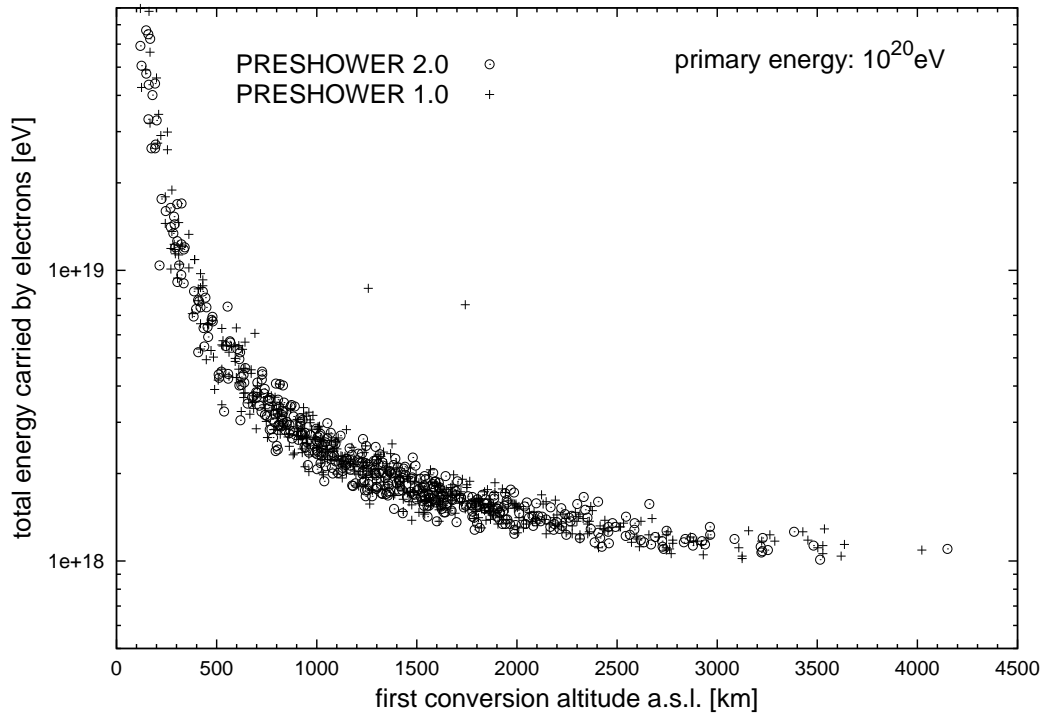


Figure 6: Energy carried by preshower electrons at the top of the atmosphere vs. the altitude of the first γ conversion for a primary photon energy of 10^{20} eV in the strong field direction. The two points in excess of the general trend are two rare cases where the first bremsstrahlung photon converted again into an electron-positron pair which increased the total energy carried by leptons. See also Fig. 5.

6. Summary

The program PRESHOWER is a tool designed for simulating magnetically induced particle cascades due to ultra-high energy photons. It can be linked with air shower simulation packages such as CORSIKA [22] to calculate complete photon-induced particle cascades as they are searched for with cosmic ray observatories.

A new version of the PRESHOWER program, version 2.0, has been released and its features are presented in this article. An efficient veto algorithm has been introduced to sample the locations of individual interaction processes. Other modifications include the update of the geomagnetic field model, correcting a rare exception, and reorganizing the program code. The results obtained with the new release of PRESHOWER agree very well with those calculated with the previous version.

The new algorithm not only speeds up the program by more than a factor 5, but also allows additional applications due to the increased flexibility of the sampling of interaction points. For example, the preshower effect can now be studied not only in the geomagnetic field, but also close to extended astrophysical objects like neutron stars and active galactic nuclei. An application of PRESHOWER 2.0 in the conditions other than the geomagnetic field require only small changes in the program. The magnetic field model has to be replaced and start and end points of simulations have to be adequately adjusted.

Acknowledgements

We thank N.A. Tsyganenko for valuable remarks on the application of the IGRF model. We are also thankful to Carla Bleve whose update of the IGRF coefficients in Tsyganenko's subroutine has been used.

This work was partially supported by the Polish Ministry of Science and Higher Education under grant No. N N202 2072 38 and by the DAAD (Germany) under grant No. 50725595.

Appendix A. Magnetic pair production: $\gamma \rightarrow e^+e^-$

The number of pairs created by a high-energy photon in the presence of a magnetic field per path length dr can be expressed in terms of the attenuation

coefficient $\alpha(\chi)$ [23]:

$$n_{pairs} = n_{photons}\{1 - \exp[-\alpha(\chi)dr]\}, \quad (\text{A.1})$$

where

$$\alpha(\chi) = 0.5(\alpha_{em}m_e c/\hbar)(B_{\perp}/B_{cr})T(\chi) \quad (\text{A.2})$$

with α_{em} being the fine structure constant, $\chi \equiv 0.5(h\nu/m_e c^2)(B_{\perp}/B_{cr})$, B_{\perp} is the magnetic field component transverse to the direction of the photon's motion, $B_{cr} \equiv m_e^2 c^3/e\hbar = 4.414 \times 10^{13}$ G and $T(\chi)$ is the magnetic pair production function. $T(\chi)$ can be well approximated by:

$$T(\chi) \cong 0.16\chi^{-1}K_{1/3}^2\left(\frac{2}{3\chi}\right), \quad (\text{A.3})$$

where $K_{1/3}$ is the modified Bessel function of order 1/3. For small or large arguments $T(\chi)$ can be approximated by

$$T(\chi) \cong \begin{cases} 0.46 \exp(-\frac{4}{3\chi}), & \chi \ll 1; \\ 0.60\chi^{-1/3}, & \chi \gg 1. \end{cases} \quad (\text{A.4})$$

We use Eq. (A.1) to calculate the probability of γ conversion over a small path length dr :

$$p_{conv}(r) = 1 - \exp[-\alpha(\chi(r))dr] \simeq \alpha(\chi(r))dr. \quad (\text{A.5})$$

Appendix B. Magnetic bremsstrahlung

After photon conversion, the electron-positron pair is propagated. The energy distribution in an e^+e^- pair is computed according to Ref. [24]:

$$\frac{d\alpha(\varepsilon, \chi)}{d\varepsilon} \approx \frac{\alpha_{em}m_e c B_{\perp}}{\hbar B_{cr}} \frac{3^{1/2}}{9\pi\chi} \frac{[2 + \varepsilon(1 - \varepsilon)]}{\varepsilon(1 - \varepsilon)} K_{2/3} \left[\frac{1}{3\chi\varepsilon(1 - \varepsilon)} \right], \quad (\text{B.1})$$

where ε denotes the fractional energy of an electron and the other symbols were explained in the previous chapter. The probability of asymmetric energy partition grows with the primary photon energy and with the magnetic field. Beginning from $\chi > 10$, the asymmetric energy partition is even more favored than the symmetric one.

Electrons traveling at relativistic speeds in the presence of a magnetic field emit bremsstrahlung radiation (synchrotron radiation). For electron

energies $E \gg m_e c^2$ and for $B_\perp \ll B_{cr}$, the spectral distribution of radiated energy is given in Ref. [25]:

$$f(y) = \frac{9\sqrt{3}}{8\pi} \frac{y}{(1 + \xi y)^3} \left\{ \int_y^\infty K_{5/3}(z) dz + \frac{(\xi y)^2}{1 + \xi y} K_{2/3}(y) \right\}, \quad (\text{B.2})$$

where $\xi = (3/2)(B_\perp/B_{cr})(E/m_e c^2)$, E and m_e are electron initial energy and rest mass respectively, $K_{5/3}$ and $K_{2/3}$ are modified Bessel functions, and y is related to the emitted photon energy $h\nu$ by

$$y(h\nu) = \frac{h\nu}{\xi(E - h\nu)}; \quad \frac{dy}{d(h\nu)} = \frac{E}{\xi(E - h\nu)^2}. \quad (\text{B.3})$$

The total energy emitted per unit distance is (in CGS units)

$$W = \frac{2}{3} r_0^2 B_\perp^2 \left(\frac{E}{m_e c^2} \right)^2 \int_0^\infty f(y) dy \quad (\text{B.4})$$

with r_0 being the classical electron radius. For our purposes we use the spectral distribution of radiated energy defined as

$$I(B_\perp, E, h\nu) \equiv \frac{h\nu dN}{d(h\nu) dx}, \quad (\text{B.5})$$

where dN is the number of photons with energy between $h\nu$ and $h\nu + d(h\nu)$ emitted over a distance dx . From Eqs. (B.2), (B.3), (B.4), and (B.5) we get¹

$$I(B_\perp, E, h\nu) = \frac{2}{3} r_0^2 B_\perp^2 \left(\frac{E}{m_e c^2} \right)^2 f(h\nu) \frac{E}{\xi(E - h\nu)^2}. \quad (\text{B.6})$$

Provided dx is small enough, dN can be interpreted as a probability of emitting a photon of energy between $h\nu$ and $h\nu + d(h\nu)$ by an electron of energy E over a distance dx . In our simulations we use a small step size of $dx = 1$ km. The total probability of emitting a photon in step dx can then be written as

$$P_{brem}(B_\perp, E, h\nu, dx) = \int dN = dx \int_0^E I(B_\perp, E, h\nu) \frac{d(h\nu)}{h\nu}. \quad (\text{B.7})$$

The energy of the emitted photon is simulated according to the probability density distribution $dN/d(h\nu)$ obtained from Eq. B.7.

¹ Expression (B.6), valid for all values of $h\nu$, is equivalent to Eq. (2.5a) in Ref. [23]. A simplified form of distribution (B.6) is given by Eq. (2.10) in Ref. [23], however it can be used only for $h\nu \ll E$.

Appendix C. Details on the new and modified files included in the PRESHOWER 2.0 package

The files included in PRESHOWER 2.0 package but not existing in the previous release are :

`IGRF-11.f` An external routine generating the geomagnetic field components according to the IGRF-11 model [2]. This file replaces `igrf.f` of the previous release of PRESHOWER.

`cernbess.f` External procedures calculating the sequence of modified Bessel functions [3]. These open source procedures replace previously used functions from Numerical Recipes.

`veto.c` This file contains functions and procedures called by the veto algorithm.

`veto.h` The header file for `veto.c`.

`utils.c` This file contains auxiliary functions and procedures used within the program. In the previous version of PRESHOWER the auxiliary functions were placed in `preshw.c`, now it is more convenient to have them in a separate file.

`utils.h` The header file for `utils.c`.

The list of files which existed in the previous release of PRESHOWER but have been modified for PRESHOWER 2.0 include:

`preshw.c` contains the main procedure `preshw_veto` generating preshowers with the veto algorithm,

`prog.c` reads input parameters and calls `preshw_veto`,

`Makefile` modified to account for the new files.

References

- [1] C. C. Finlay et al., *Geophys. J. Int.*, 183, (2010), 1216, doi: 10.1111/j.1365-246X.2010.04804.x, <http://www.ngdc.noaa.gov/IAGA/vmod/igrf.html>

- [2] N. A. Tsyganenko, Institute and Department of Physics, Saint-Petersburg State University, Russia, private communication; <http://geo.phys.spbu.ru/~tsyganenko/Geopack-2008.html>
- [3] <http://wwwasdoc.web.cern.ch/wwwasdoc/shortwrupsdir/c341/top.html>
- [4] Numerical Recipes, <http://www.nr.com>
- [5] J. Blümer, R. Engel, and J. R. Hörandel, Prog. Part. Nucl. Phys. **63** (2009) 293
- [6] A. Letessier-Selvon and T. Stanev, Rev. Mod. Phys. **83** (2011) 907
- [7] K. Kotera, and A. V. Olinto, Ann. Rev. Astron. Astrophys. 49 (2011) 119, arXiv:1101.4256
- [8] J. Abraham *et al.* (Pierre Auger Collaboration), Nucl. Instrum. Meth. A 523 (2004), 50
- [9] H. Tokuno *et al.*, (TA Collaboration) AIP Conf. Proc. **1238** (2010) 365
- [10] B. McBreen and C. J. Lambert, Phys. Rev. D **24**, (1981) 2536
- [11] P. Homola *et al.*, Comp. Phys. Comm. 173 (2005) 71
- [12] M. Risse and P. Homola, Mod. Phys. Lett. A 22 (2007), 749
- [13] S. Karakula and W. Bednarek, Proc. 24th Int. Cosmic Ray Conf., Rome, (1995) 266
- [14] T. Stanev and H. P. Vankov, Phys. Rev. D **55** (1997) 1365
- [15] X. Bertou, P. Billoir and S. Dagoret-Campagne, Astropart. Phys. **14** (2000) 121
- [16] W. Bednarek, New Astron. **7** (2002) 471
- [17] H. P. Vankov, N. Inoue, and K. Shinozaki, Phys. Rev. D **67** (2003) 043002
- [18] H. P. Vankov *et al.*, Proc. 28th Int. Cosmic Ray Conf., Tsukuba, (2003) 527

- [19] T. Sjöstrand et al., arXiv:hep-ph/0308153v1 (2003)
- [20] T. Stanev et al., Phys. Rev. D62, 093005 (2000)
- [21] <http://www.ngdc.noaa.gov/IAGA/vmod/igrf.html>
- [22] D. Heck, J. Knapp, J. N. Capdevielle, G. Schatz, and T. Thouw, Report FZKA 6019, Forschungszentrum Karlsruhe, 1998 (available at www-ik.fzk.de/~heck/corsika/)
- [23] T. Erber, Rev. Mod. Phys. **38** (1966) 626
- [24] J. K. Daugherty, A. K. Harding, Astrophys. J. **273** (1983) 761
- [25] A. A. Sokolov, I. M. Ternov, Radiation from Relativistic Electrons, Springer Verlag, Berlin, 1986